

Structural evolution of Fe-18Ni-16Cr-4Al steel during aging at 950 °C

Man Wang^{a,b}, Zhangjian Zhou^b, Jinsung Jang^{a*}

^a Nuclear Materials Development Div., KAERI, Daejeon, Korea

^b School of Materials Science and Engineering, USTB, Beijing, China

*Corresponding author: jjang@kaeri.re.kr

1. Introduction

Motivation to improve the efficiency of power plants has received much attention, especially after CO₂ emission issue. The efficiency of power plants depends on the operating temperature and pressure [1]. However increasing the operating parameters makes the service conditions severer for the key components and demands stronger structural materials with better high temperature creep properties and oxidation resistance.

Austenitic stainless steels are also among important structural materials for in-core components of nuclear reactors, and the performance, the oxidation resistance as well as the mechanical strength at high temperature are further expected after Fukushima accident. Alumina-forming austenitic (AFA) steel was first developed by Y. Yamamoto et al. [2], which showed a good combination of oxidation resistance and creep resistance. The strengthening is achieved through nano-sized MX and Laves [3,4]. This kind of material is expected to be used for 10⁵ h and the long term stability of grain structure and precipitates shall be critical to the performance. In this study, the structural evolution of a new austenitic stainless steel during aging at 950 °C is investigated.

2. Material and Experimental

Chemical composition of the experimental steel was designed as Fe-18Ni-16Cr-2Mo-0.3Si-4Al-0.4Nb-0.2Y-0.01B in weight percent. The steel was fabricated by vacuum induction melting, followed by forging and hot rolling. Samples were cut from the rolled sheet and solution treated at 1200 °C for 30 mins. Then cold rolling with a reduction of 7% was applied to the samples. Aging treatment was conducted at 950 °C for 10 h, 50 h and 100 h respectively. To retain the aging structure, samples were water quenched after aging.

Microstructural evolution was observed by using scanning electron microscopy and high-resolution transmission electron microscopy.

3. Results and Discussion

3.1 Microstructural Evolution

Fig. 1 shows the microstructural evolution of matrix during aging at 950 °C. After solution treatment at 1200 °C, the sample appears to consist of two phase, austenite (γ) and ferrite (α). As shown in Fig.1 (a), there

are round particles dispersed in ferrite (marked as region ①), while there are no precipitates in austenite (marked as region ②). In austenitic matrix most precipitates seem to be dissolved at the solution treatment temperature. After aging at 950 °C for 10 h, needle-shaped precipitates began to occur in austenite, as indicated by the red arrow in Fig.1 (b). Along with the aging time, there occur more needle-shaped precipitates, as shown in Fig.1 (c) and (d). Also it can be seen clearly that the round particles dispersed in ferrite matrix get coarsen.

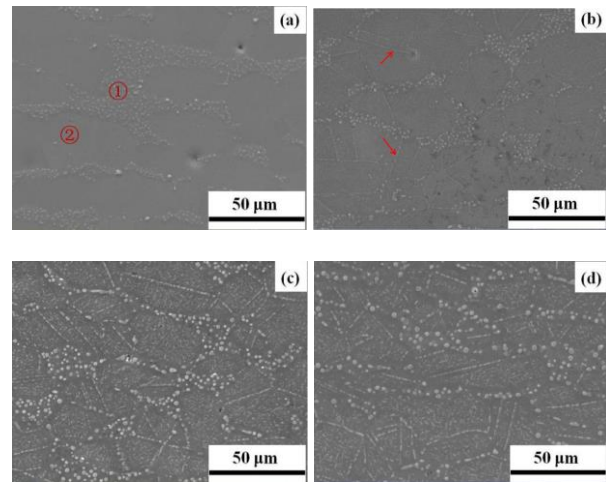


Fig.1 The microstructure of matrix during annealing (a) as solid solution (b) 950 °C, 10h (c) 950 °C, 50h (d) 950 °C, 100h

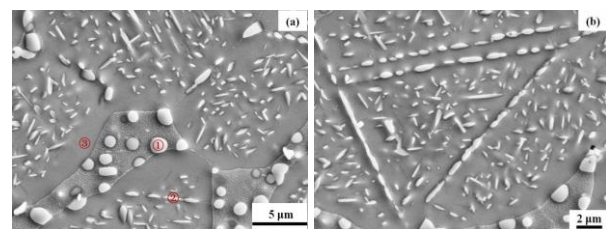


Fig.2 The precipitates after aging at 950 °C for 50h (a) precipitates in the matrix (b) needle-shaped precipitates

Table I: EDS results of precipitates in Fig.2 (a) (at. %)

region	Fe	Cr	Ni	Al	Si
①-round particle	20.3	5.6	37.9	36.2	-
②-needle precipitate	46.0	13.2	23.6	17.2	-
③-matrix	60.0	17.6	15.6	5.7	1.1

Fig.2 shows the morphologies of precipitates after aging at 950 °C for 50 h. According to the EDS results

(as shown in Table I), both round particles and needle-shaped precipitates are enriched with Al and Ni, compared with the matrix. It seems that there are relatively higher contents of Fe and Cr in the needle-shaped precipitates. Due to the needle shape of the precipitates, it is inevitable that the EDS results contain the information from the matrix. It can be seen clearly that some of the needle-shaped precipitates are aligned in certain orientation as shown in Fig.2 (b). Moreover, fine round particles with size of about 100 nm are dispersed in ferrite matrix.

3.2 Characterization of Precipitates

Fig.3 shows the TEM images of round particles. According to the EDS and SADP, nano-sized round particle is characterized to be NiAl and it disperses in the phase of ferrite.

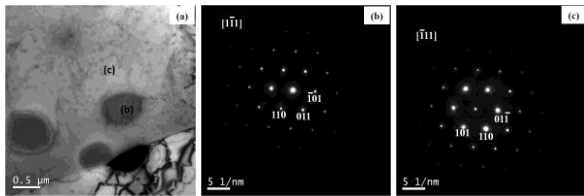


Fig.3 TEM images of round particles in the matrix (a), diffraction pattern of round particle (b) and diffraction pattern of matrix (c)

Table II: EDS results of precipitates in Fig.3 (a) (at. %)

region	Fe	Cr	Ni	Al	Mo
(b)-round particle	26.4	7.0	41.3	24.1	0.4
(c)-matrix	37.1	62.9	-	-	-

Fig.4 shows the morphology of matrix where the needle-shaped precipitates disperse. This matrix is characterized to be austenite, as shown in Fig.4 (b). The needle-shaped precipitate is also NiAl and Fig.5 (b) is the SADP under zone axis of [001]. Although a high content of C was found in the needle-shaped precipitate in Fig.5 (a), it shall be investigated in more detail in the future.

Based on the TEM results, both round particles and needle-shaped precipitates are characterized to be NiAl. Different precipitate shapes are resulted from differences in structural parameters as shown in Table IV. The lattice misfit of NiAl to ferrite is about 0.4%, while 19.6% to austenite. When NiAl precipitates in ferrite, interface energy would be more important since the distortion energy caused by lattice misfit is very small. Therefore the precipitates become in round shape in ferrite. However, the distortion energy becomes more critical when it precipitates in austenite because of the high misfit. Therefore they precipitate in needle shape in austenitic phase.

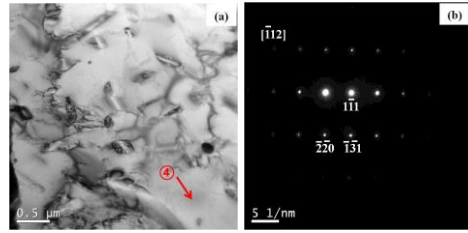


Fig.4 TEM images of needle-shaped precipitates in the matrix (a) and diffraction pattern of the matrix (b)

Table III: EDS results of needle-shaped precipitates in Fig.4 (a) and Fig.5 (a) (at. %)

region	Fe	Cr	Ni	Al	Co	C
④	41.2	56.0	2.8	-	-	-
⑤	28.2	6.6	20.1	11.0	3.1	31.0

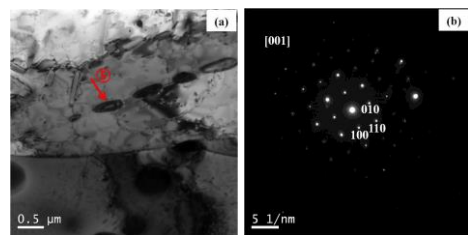


Fig.5 TEM image of needle-shaped precipitates (a) and its diffraction pattern (b)

Table IV: Structural parameters of precipitates and matrix

type	structure	parameters
NiAl	Cubic $\text{Pm}\bar{3}\text{m}(221)$	$a=b=c=2.888\text{\AA}$, $\alpha=\beta=\gamma=90^\circ$
Ferrite-bcc	Cubic $\text{I}\text{m}\bar{3}\text{m}(229)$	$a=b=c=2.876\text{\AA}$, $\alpha=\beta=\gamma=90^\circ$
Austenite-fcc	Cubic $\text{Fm}\bar{3}\text{m}(225)$	$a=b=c=3.591\text{\AA}$, $\alpha=\beta=\gamma=90^\circ$

4. Conclusions

Microstructural evolution of Fe-18Ni-16Cr-4Al during aging at 950 $^\circ\text{C}$ was studied. This steel consists of two phases of austenite and ferrite. During aging, needle-shaped NiAl precipitates in austenite, while round shaped NiAl form in ferrite, which is supposed to be due to different crystal structural parameters.

REFERENCES

- [1] R. Viswanathan and W. Bakker, Materials for Ultrasupercritical Coal Power Plants-Boiler Materials: Part 1, Journal of Materials Engineering and Performance, Vol. 10(1), p. 81, 2001.
- [2] Y. Yamamoto, M.P. Brady, Z.P. Lu, P.J. Maziasz, C.T. Liu, B.A. Pint, K.L. More, H.M. Meyer and E.A. Payzant, Creep-Resistant, Al_2O_3 -Forming Austenitic Stainless Steels, Science, Vol. 316, p. 433, 2007.
- [3] Y. Yamamoto, M.P. Brady, Z.P. Lu, C.T. Liu, M.Takeyama, P.J. Maziasz and B.A. Pint, Alumina-Forming

Austenitic Stainless Steels Strengthened by Laves Phase and MC carbide Precipitates, *Metallurgical and Materials Transactions A*, Vol. 38A, p. 2337, 2007.

[4] D.Q. Zhou, W.X. Zhao, H.H. Mao, Y.X. Hu, X.Q. Xu, X.Y. Sun and Z.P. Lu, Precipitate Characteristics and Their Effects on the High-Temperature Creep Resistance of Alumina-Forming Austenitic Stainless Steels, *Materials Science & Engineering A*, Vol. 622, p. 91, 2015.